ACS OMEGA

Open Access

http://pubs.acs.org/journal/acsodf

Article

Injectable Chitosan−Methoxy Polyethylene Glycol Hybrid Hydrogel Untangling the Wound Healing Behavior: In Vitro and In Vivo Evaluation

Fizza Mushtaq,[#] Madeeha Ashfaq,[#] Fareeha Anwar,[*] Badarqa Tul Ayesha, Hafiz Shahid Latif, Sadia Khalil, Hafiz Shoaib Sarwar, Muhammad Imran Khan, Muhammad Farhan Sohail, and Iram Maqsood[*]

Cite This: *ACS Omega* 2024, 9, 2145−2160

Read Online

ACCESS | Metrics & More | Article Recommendations

ABSTRACT: Wound healing, particularly for difficult-to-treat wounds, presents a serious threat and may lead to complications. Currently available dressings lack mucoadhesion, safety, efficacy, and, most importantly, patient compliance. Herein, we developed a unique, simple, and inexpensive injectable chitosan−methoxy polyethylene glycol (chitosan−mPEG) hybrid hydrogel with tunable physicochemical and mechanical properties for wound healing. The detailed physicochemical and rheological characterization of the chitosan−mPEG hydrogel has revealed chemical interaction between available $-NH_2$ groups of chitosan and −COOH groups of mPEG acid, which, to our perspective, enhanced the mechanical and wound healing properties of hybrid chitosan and mPEG hydrogel compared to solo chitosan or PEG hydrogel. By introducing mPEG, the wound healing ability of hydrogel is synergistically improved due to its antibacterial feature, together with chitosan's innate role in hemostasis and wound closure. The detailed hemostasis and wound closure potential of the chitosan−mPEG hydrogel were investigated in a rat model, which confirmed a significant acceleration in wound healing and ultimately wound closure. In conclusion, the developed chitosan−mPEG hydrogel met all the required specifications and could be developed as a promising material for hemostasis, especially wound management, and as an excellent candidate for wound healing application.

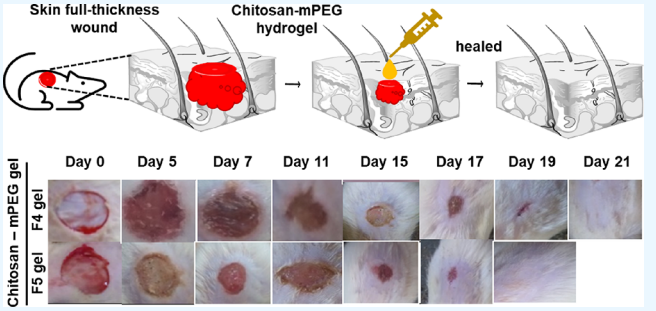

1. INTRODUCTION

Wound healing is among the complex processes in the human body that requires the synchronization of several functions, including hemostasis, inflammation, growth, re-epithelialization, and remodeling of skin tissues.[1] All the steps in ordered stages are regulated by cellular and biochemical events.[2] In addition, it includes various types of cells such as platelets, fibroblasts, and immune cells and biochemical substances.[2] Acute wounds heal over time following a normal healing process and pose no severe concerns in therapeutics.[3] However, chronic and difficult-to-treat wounds fail to proceed through an orderly and timely process, resulting in complex treatment plans requiring extended hospitalization and economic burden. Usually, chronic wounds, classified as pressure ulcers, arterial or venous ulcers, and diabetic ulcers, are generally associated with patients having compromised health conditions such as obesity, diabetes, or geriatrics. The mechanism of chronic wounds is still unclear as they do not follow the normal healing process and remain in the inflammation phase, further worsened by bacterial colonization, ischemia, aging, and reperfusion injury.[3] Even though wound treatment or management is performed by several methods, a previous study confirmed that moist wound dressing accelerates the healing process.[4]

An ideal wound dressing should absorb and remove the exudate, prevent microbial infection, and protect the wound from the external environment. Moreover, these dressings can promote wound healing by preventing fluid loss and epithelial reconstruction, maintaining a favorable environment while adhering to the wound area and permitting easy removal for patients. Thus, the dressing must be designed as a porous material for proper air exchange and protecting the wounds from infection and dehydration. Previous studies have also

Received: July 12, 2023
Accepted: September 22, 2023
Published: December 29, 2023

confirmed that moist wound dressing accelerates the healing process.[4] Based on our previous expertise, the hydrogel is a moist wound healing material made up of synthetic and natural polymers.[5] On the other hand, hydrogel as an extracellular matrix (ECM) mimics a three-dimensional (3D), porous cell culture platform that holds an excellent safety profile[6] and forms a hemostatic plug or physical barrier at the bleeding site.[7]

Hydrogels are polymeric matrices that expand but do not dissolve in water.[8] The swelling property is due to this class of materials' significant thermodynamic affinity for the solvent. This property, with characteristics of adaptability and tunability of the material, has led to substantial studies and benefits of hydrogels in recent years. For form and mechanical strength, the network achieves equilibrium with the liquid and temperature of its surroundings. Variations in the polymer's structure, concentration, and functionality and/or the cross-linker utilized in such gels can alter the hydrogel's structure.[9] Besides conventional hydrogel, injectable hydrogel is an *in situ* gelling system, since injectability dictates improved gelation kinetics control with considerable alleviation of patients' discomfort and pain associated with invasive surgery while shortening the healing time, and it is applied to irregularly shaped tissues in addition to hard-to-reach tissue sites.[10,11] It has been reported extensively in literature that hydrogel is fabricated from natural polymers and synthetic polymers.[12,13] However, although natural hydrogels and synthetic hydrogels are widely used in wound healing and wound management due to their exceptional advantages, both of these hydrogel systems possess limitations in their respective domains.[14] In order to overcome these limitations, we are introducing here an alternative strategy by developing a hydrogel by a combination of natural and synthetic polymers in order to achieve unique benefits from both kinds of polymers while circumventing their individual disadvantages. Such a strategy requires a thorough screening of available natural and synthetic polymers with the intention of developing a unique, feasible, and best-suitable hybrid hydrogel by mixing a natural and a synthetic polymer together. Inspired by the idea of hybrid hydrogel, here we adopted chitosan, a natural polymer, and poly(ethylene glycol) (PEG), a synthetic polymer, as hydrogel precursors.

Compared to synthetic polymers, natural polymers are preferred for hydrogels because of their low toxicity, excellent biocompatibility, ease of degradation, rich source, and low cost.[15,16] Chitosan, a natural amino polysaccharide, contains various reactive functional groups, including amine and hydroxyl, which form hydrogels through chemical cross-linking.[17,18] It is also reported that chitosan can perform many therapeutic actions like anti-inflammatory, antibacterial, hemostatic, wound healing, and antioxidant activities.[19] Chitosan, a natural biopolymer, plays a significant role in wound healing due to its outstanding bioadhesive, hemostatic, anti-inflammatory, antimicrobial, and tissue regeneration properties.[20] Administration of chitosan in hydrogels is also of great interest nowadays because of its self-healing characteristics.[21]

Based on previous expertise, we have introduced methoxy polyethylene glycol (mPEG) as the second important component of injectable optimized hybrid hydrogel together with chitosan for animal wound healing. Methoxy-PEG is a nonionic, nontoxic, nonimmunogenic polymer that has been used to suppress host immunity together with acceleration of adipogenesis.[22,23] Besides that, PEG has also been reported as an injectable hydrogel precursor for controlled drug release, hemostasis, and wound healing applications.[24,25] To the best of our knowledge, hydrogel formulations for wound healing applications necessitate incorporation of an antibacterial agent or drug to kill the microbes at the wound site; however, most of the antimicrobial agents lack broad-spectrum activity together with burst release of drug at the wound site. This could lead to discomfort and harmful effects to patients due to abrupt release and exposure to high drug concentrations. In contrast, here we proposed to develop an ideal hybrid hydrogel from two components, namely, chitosan and mPEG, which both possess inherent strong antibacterial properties required for wound healing applications.[25−27]

In this context, the present study was designed to fabricate a chitosan−mPEG hybrid hydrogel using a range of different concentrations of chitosan that are cross-linked subsequently with methoxy polyethylene glycol acid as a potential wound healing material. The fabricated hydrogels are further characterized in detail, including rheological evaluation as well as swelling behavior, leachability, cytocompatibility, antibacterial activity, and *in vitro* degradation of the hydrogel. Later, we investigate in detail the potential of developed and fully characterized promising chitosan−mPEG hydrogels in wound healing as well as the acceleration of wound closure in animal rat models.

2. RESULTS AND DISCUSSION

Wounds are skin defects and, therefore, need proper treatment. Wound healing is a physiological skin repairing activity that consists of four distinctive phases, hemostasis, inflammation, proliferation, and maturation. All healing stages are cellular (RBCs, platelets, neutrophils, macrophages, etc.) and biochemical (involvement of fibroblast, chemotactic factors, growth factors, and collagen deposition) responses. A previous study confirmed that moist wound dressing accelerates the healing process.[4] To this end, hydrogels are an ideal option because hydrogels with natural polymers like chitosan, collagen, and alginate are recommended for wound management as they mimic or possess similar properties of the natural tissue matrix. It is reported that chitosan, being a natural polycationic biopolymer, is embodied with wound healing properties. Simultaneously, as a second hydrogel-forming material, we have introduced mPEG, which is nontoxic and possesses wound healing attributes. Chitosan and PEG hydrogels are extensively investigated for numerous pharmaceutical purposes. A recent advancement has been developed with the instigation of injectable hydrogels, which are more beneficial and effective than conventional topical hydrogels. In this context, the present study aims to develop injectable chitosan−mPEG hybrid hydrogels and, subsequently, to evaluate the wound healing potential of the chitosan−mPEG hybrid hydrogel at excised acute wounds in experimental rats (Figure 1).

2.1. Formation and Characterization of Injectable Chitosan−mPEG Hybrid Hydrogels. At least five batches of hydrogels containing different concentrations of chitosan but with similar chitosan and mPEG−COOH ratios, namely, F1, F2, F3, F4, and F5 (Table 1), were fabricated in a reproducible manner with regard to formation of intact gels. However, of the five batches, the last two (F_4 and F_5) hydrogels were considered best among all and used for further detailed characterization and animal studies. We postulate that the injectable chitosan−mPEG hybrid hydrogel was prepared in

https://doi.org/10.1021/acsomega.3c04346
ACS Omega 2024, 9, 2145−2160

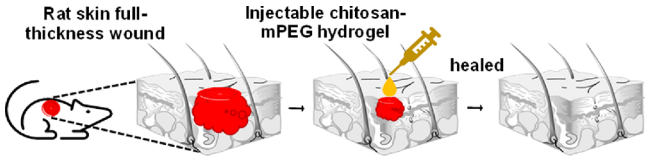

Figure 1. Illustrations showing the acceleration in wound closure and complete wound healing upon application of injectable chitosan-mPEG hydrogel to rat skin full-thickness wound.

this study by the amide bond reaction between the chitosan and cross-linker mPEG−COOH, as illustrated in Figure 2.

In order to completely characterize the fabricated chitosan−mPEG hybrid hydrogels, different studies including studies on the rheological behavior, leachability, swelling ratio, FTIR, TGA, cytocompatibility, antibacterial activity, and *in vitro* degradation were performed.

It is well understood that the capacity of the hydrogel to sustain mechanical stress to some extent determines the scope of material applications. As a result, substantial emphasis has been placed on the investigation of the rheological features of hydrogels. On the other hand, the study of hydrogels' rheological behavior allows for the evaluation of their structural properties. By establishing a link between deformation or flow and applied stress, rheology may be utilized to identify the rheological characteristics of injectable hydrogels. A time sweep rheology was conducted (Figure 3A). Gelation was evidenced by a gradual increase of storage modulus or elastic modulus (G') and a decrease of loss modulus or viscous modulus (G'') with time.[28] With the increase in time, the loss modulus (G'') decreased and crossed over the storage modulus at a certain point, which defines the sol−gel transition curve. The sol−gel transition point for F4 was achieved earlier than for F5 at a temperature of 37 °C. The sol−gel transition of chitosan−mPEG was also dependent on the solution pH. Figure 3B shows that the storage modulus (G') slightly increases and remains unchanged with time by increases in temperature at pH 4.5 and 5.0 while the sol−gel transition is not observed at these pH values. At pH 7.0, a significant increase in storage modulus and sol−gel transition occurred in 5 min at 36−37 °C and the corresponding storage modulus was 60 times higher than that of pH 4.5 and 5.0.[29] The appearance of gels of different pH values at 37 °C was observed as shown in Figure 3E. At pH 4.5 and 5.0, the solution exists in a transparent yellowish sol state. As pH increased to 7.0, the solution underwent a sol−gel transition and became a stationary, nonflowing gel. Rheological properties including storage modulus and loss modulus of thermoresponsive gelation of chitosan−mPEG gels were measured to fully characterize the hydrogels and understand the effect of cross-linking of the resultant hydrogel properties. As previously stated, the storage modulus may be thought of as a measure of the degree of hydrogel formation; the higher the G' value of the gel, the greater the gel strength, while the elastic modulus of a gel system corresponds with the network's rigidity (stiffness), where G'' is independent of shearing time.[30] The mPEG polymer, as a cross-linker, is frequently employed to improve the rheological characteristics of thickening systems and is chosen as a thickener to explore the rheological behavior of copolymer hydrogels.[30] The flow properties (viscosity) with the shear rate for hydrogels are illustrated in Figure 3C. The variation in viscosities over time at fixed temperature values of 10 and 37 °C was conducted for both F4 and F5 hydrogels (Figure 3D). It was found that gels with a higher degree of cross-linking agent gelled faster than those with a low cross-linking polymer. This study indicates that the elastic response of the material is stronger than its viscous response. The existing hydrogel system predominantly exhibits a solid-like behavior, and this type of dynamic response is characteristic of a gel-like material.[28] It is used in a variety of applications, ranging from cosmetics to pharmaceuticals, for emulsification, stabilization, and rheological control.

The capacity of a hydrogel to expand in bulk and disintegrate over time is measured by its swelling. We measured the swelling behavior of the F4 and F5 hydrogels in this work. Both hydrogels were studied in triplicate (F4 and F5). Figure 4A and B depicts the dried hydrogel in its initial condition and the hydrogel after being immersed in PBS in its equilibrium swelling state. The swelling ratio of injectable hydrogels was evaluated over time, as shown in Figure 4C. Initially, the rate of water uptake increases until the constant swelling ratio is achieved after 48 h. The F5 sol−gel has a swelling ratio of 89.7% while the F4 sol−gel shows a swelling ratio of 85.6%, which was incredibly significant to use therapeutically. The most critical characteristics that determine the release patterns of solvents and drugs from such polymeric networks are the rate and extent of hydrogel swelling. As a result, several studies focused on providing a detailed explanation of hydrogel behavior and a mathematical description of equilibrium swelling, as well as dimensional changes owing to solvent absorption, desorption, and drug release patterns.[31,32] We performed the leaching study of both F4 and F5 chitosan−mPEG hydrogels according to the method as defined above. The comparison of both hydrogels is illustrated in Figure 4D, and it shows that both hydrogels have a significant leachable property. The leaching factor for sol−gel was found to be about 1.0, which makes it therapeutically active and can be used for medicinal purposes.

FTIR analysis was also performed to identify the functional groups present in mPEG acid, pure chitosan, and the chitosan−mPEG hydrogel. The FTIR spectra show that

Table 1. Preparation of Chitosan−mPEG Hybrid Hydrogel with Different Concentrations of Chitosan and mPEG, Hydrogel Composition, and *In Vitro* Characterization

	chitosan−mPEG hydrogel			*in vitro* characterization					
	chitosan stock solution (g)	chitosan:mPEG	hydrogel (% w/w)	rheology	swelling	leachability	FTIR, TGA	cytocompatibility, antibacterial activity	*in vitro* degradation
F1	0.12	15:1	1.0						
F2	0.18	15:1	1.5						
F3	0.21	15:1	1.8						
F4	0.25	15:1	2.0	+	+	+	+	+	+
F5	0.30	15:1	2.5	+	+	+	+	+	+

https://doi.org/10.1021/acsomega.3c04346
ACS Omega 2024, 9, 2145−2160

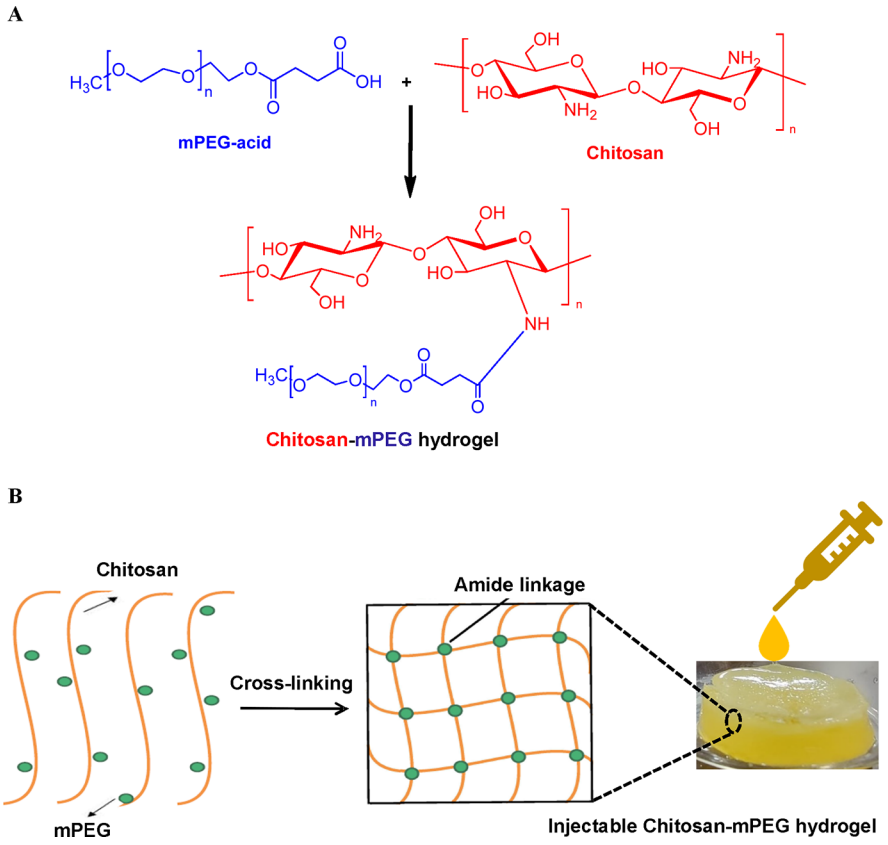

Figure 2. (A) Chemical representation of chitosan and methoxy polyethylene glycol (mPEG) reaction yielding chitosan−mPEG hybrid hydrogel *via* amide bond formation. (B) Illustration of the chitosan−mPEG hydrogel formation process.

there is formation of amide linkage between the chitosan and mPEG (Figure 5). The spectrum of mPEG shows that there is an −OH stretch at the 3500 cm^{-1} peak. The peak at 2878 cm^{-1} shows the −C−C− stretch, and the peak at 1150 cm^{-1} shows the −C−O−C− stretch. The spectrum of pure chitosan shows the presence of the −OH stretch at 3450 cm^{-1}. Peaks at 1655/1560 cm^{-1} show the amide linkage, which is further formed between the hydrogel during the reaction between chitosan and mPEG acid. Peaks at 1150/1050 cm^{-1} show the −C−O−C− stretch. All these spectra showed no change in chemical structure before, during, and after the formation of hydrogels except the formation of amide linkage between the chitosan and mPEG cross-linker, which is the key point for sol−gel formation. The distinctive peaks of the chitosan−mPEG hydrogel spectrum were identical to those of its parent polymers. Figure 5 shows that the distinctive adsorption of chitosan at 1050, 1150, 1560, 1655, and 3450 cm^{-1} corresponds to the glycosidic linkage (−C−O−C−) inside and between monomers as well as to the amide II band, the amide I band, and the internal hydroxyl group. The spectra of the chitosan−mPEG hydrogel showed peaks identical to those of chitosan as well as the adsorption of carbonyl groups at about 1740 cm^{-1}. Furthermore, the amide I and II bands were more intense in the chitosan−mPEG hydrogel than in chitosan. The rise in amide I and amide II bands elucidates the creation of an amide bond between chitosan and mPEG acid, culminating in an injectable chitosan−mPEG hydrogel.

The TGA thermograms of chitosan, mPEG acid, and chitosan−mPEG hydrogel are shown in Figure 6. As expected, all three materials chitosan, mPEG acid, and chitosan−mPEG hydrogels exhibited weight loss starting at 85 °C, which could be due to water loss, in agreement with Yang.[33] Typically, chitosan demonstrated a two-step degradation process where rapid weight loss was observed between 60 and 140 °C, which is believed to be caused by sugar unit dehydration and bond cleavage of the primary chain. The final weight loss for chitosan was found to be above 300 °C, which would possibly be due to serious pyrolysis. Besides that, mPEG represented a clearly distinct pattern of weight loss that also consisted of two main phases, one of which occurred between 80 and 120 °C while the second weight loss was observed at approximately 380 °C. On the contrary, the chitosan−mPEG hydrogel exhibited a totally different pattern of weight loss as compared to chitosan or mPEG thermograms. Briefly, the chitosan−mPEG hydrogel exhibited a three-step weight loss pattern; the first out of three rapid weight losses occurred between 100 and 220 °C, the second out of three weight losses showed at 410 °C, and the final slight weight loss was found at 520 °C. Overall, we believe that the mPEG-cross-linked chitosan hydrogel exhibited better thermal stability than the solo chitosan or mPEG acid.

2.2. Cytocompatibility and Antibacterial Activity of Chitosan−mPEG Gels. In this study, the cytocompatibility of chitosan−mPEG hydrogels embedded with L929 mouse fibroblasts was explored using the WST-8 assay (Figure 7, left). According to expectation, the injectable chitosan−mPEG hydrogel was well tolerated by L929 fibroblasts, which represented cell proliferation over time. It was interesting to find that cell viability in both cell-laden hydrogels declined on the second day,[33] which is likely due to the effect of trypsinization and stress during encapsulation. However, the encapsulated cells continued to grow and a significant increase

https://doi.org/10.1021/acsomega.3c04346
ACS Omega 2024, 9, 2145−2160

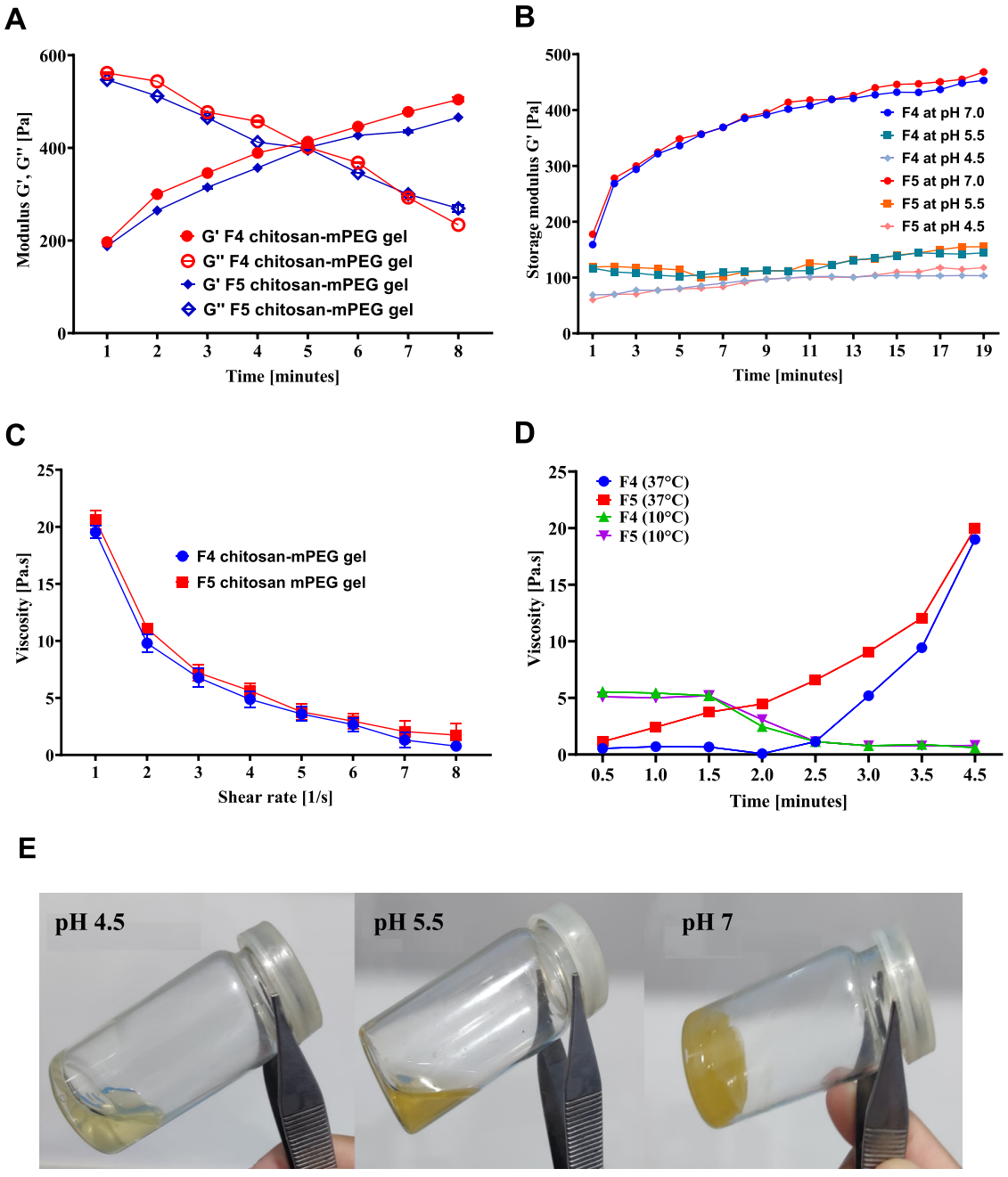

Figure 3. (A) Time sweep rheology of hydrogels. (B) Rheological characterization at different pH values of chitosan−mPEG injectable hydrogels. (C) Stress strain rheological study of F4 and F5 hydrogels against viscosity. Data points with error bars represent means ± standard deviations (n = 3). (D) Viscosity changes of chitosan−mPEG hydrogels (F4, F5) as a function of time at temperatures 10 and 37 °C. (E) Physical appearance of chitosan−mPEG hydrogels at various pH values. Photograph courtesy of "Iram Maqsood". Copyright 2023.

in cell viability was found on day 3. It is important to mention here that cell viability in hydrogels was more or less comparable to 2D cell viability. Besides that, the blank chitosan−mPEG hydrogels (without cells) have also somehow reduced yellow WST-8 dye to orange WST-8 formazan, which we assume that tetrazolium dye absorbed at the chitosan surface and thereby reduced. Taken together, chitosan−mPEG hydrogels showed improved cell growth and cell viability and demonstrated good cell biocompatibility.

The antibacterial activity of the chitosan−mPEG hydrogel was evaluated against *Escherichia coli*by the agar well diffusion method, as represented in Figure 7 (right). The pure chitosan as well as chitosan−mPEG hydrogels induced the measurable zone of inhibition formation, while distilled water, used as a negative control, showed no inhibition zone formation according to expectation. It is important to highlight here that chitosan significantly inhibited the growth of bacteria as compared to negative control while both chitosan−mPEG hydrogels showed a superior antibacterial effect as compared to chitosan against *E. coli*after 24 and 48 h. This possible mechanism can be attributed to the fact that the antibacterial activity of chitosan is due to its polycationic structure that caused a strong electrostatic interaction with a negatively charged cell surface of bacteria leading to cell membrane disturbance and consequently leakage and bacterial death. Besides that, the superior antibacterial activity of the chitosan−

https://doi.org/10.1021/acsomega.3c04346
ACS Omega 2024, 9, 2145−2160

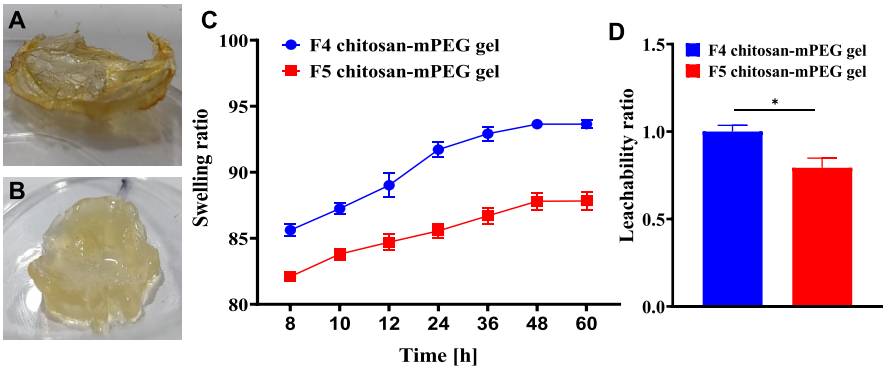

Figure 4. Swelling ability of hydrogel from (A) a dried state to (B) a swelling state after immersing it in phosphate-buffered saline solution for 48 h. (C) Swelling study of F4 and F5 hydrogels against time in phosphate-buffered saline solution (pH 7.4) for 2 days. Data points with error bars represent means ± standard deviations. (D) Comparison of the leachable behavior of the F4 and F5 chitosan−mPEG injectable hydrogels. Columns with error bars represent means ± standard deviations (n = 3). Columns with asterisk (*) are statistically significantly different (P < 0.05). Photograph courtesy of 'Iram Maqsood and Fizza Mushtaq'. Copyright 2023.

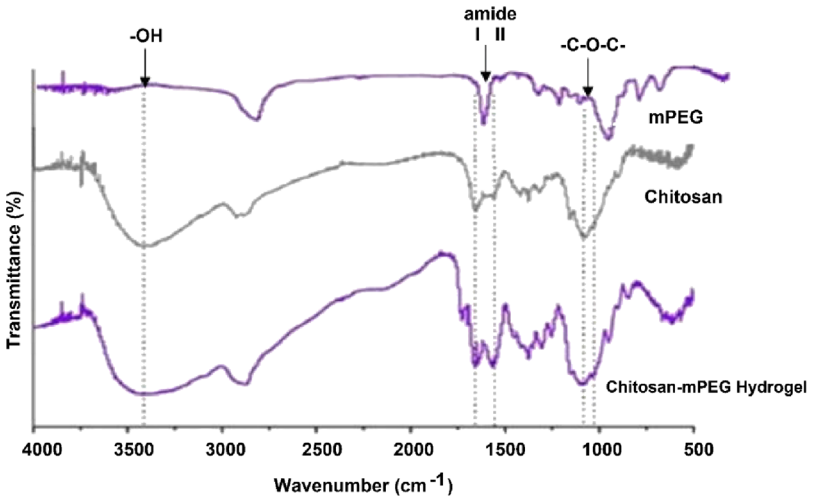

Figure 5. FTIR spectra of the mPEG acid, chitosan, and chitosan−mPEG injectable hybrid hydrogel.

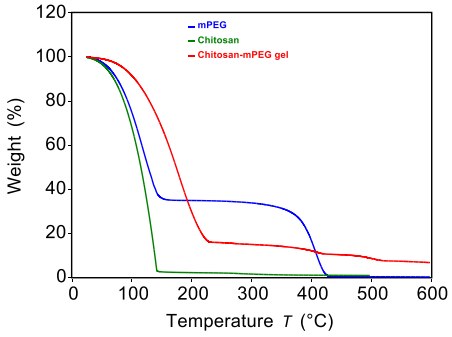

Figure 6. TGA thermograms of chitosan, mPEG acid, and chitosan−mPEG hydrogel.

mPEG hydrogel to that of chitosan could be explained by the observation that the presence of mPEG in the hydrogel formulation synergistically increases the antibacterial effect of hydrogel than chitosan only. Broadly speaking, this study confirmed that mPEG has itself a certain antibacterial effect against *E. coli*, which was in concordance with Liu, who discovered the antibacterial effect of injectable PEG hydrogel against Gram-positive and Gram-negative bacteria without the addition of an antibiotic.[26] Altogether, we believe that the excellent antibacterial activity of the chitosan−mPEG hydrogel will be subjected to further improvement for biomedical application.

An *in vitro* degradation study of chitosan−mPEG hydrogels was performed for 4 weeks. A degradation study of both F4 and F5 hydrogels was conducted *in vitro* by incubating the samples in phosphate-buffered saline at pH 7.4 at 37 °C. Different parameters such as pH, weight after the immersion time (Wt), and dry gel weight (Wo) were measured at each time point. After the first week, the pH of each sample was checked with the help of a pH meter and data was recorded. After 7 days, another sample from each hydrogel was taken and the degradation index was calculated. The same procedure was repeated during the 14 days of study to estimate the degradation index against each hydrogel as above. The pH, initial weight, and weight after immersion were measured to calculate the degradation index. At 21 days of degradation study, it was observed that all the hydrogels remained resistant to environmental conditions and no hydrogel was completely dissolved in the phosphate-buffered saline during study. A study was also conducted to evaluate the degradation at 28 days of study. After 28 days of study, it was observed that some hydrogels were somewhat disintegrated in the phosphate saline at different pH. The pictorial illustration of all these samples (F4 and F5) after every week of study is shown in Figure 8.

https://doi.org/10.1021/acsomega.3c04346
ACS Omega 2024, 9, 2145−2160

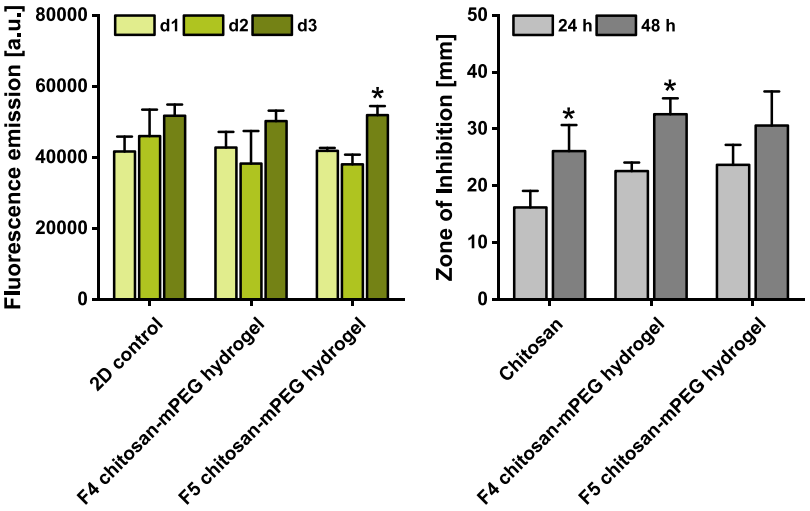

Figure 7. (Left) Cytocompatibility study and (right) antibacterial study of chitosan−mPEG hydrogels. Columns with asterisk (*) are statistically significantly different than on day 1 ($P < 0.05$).

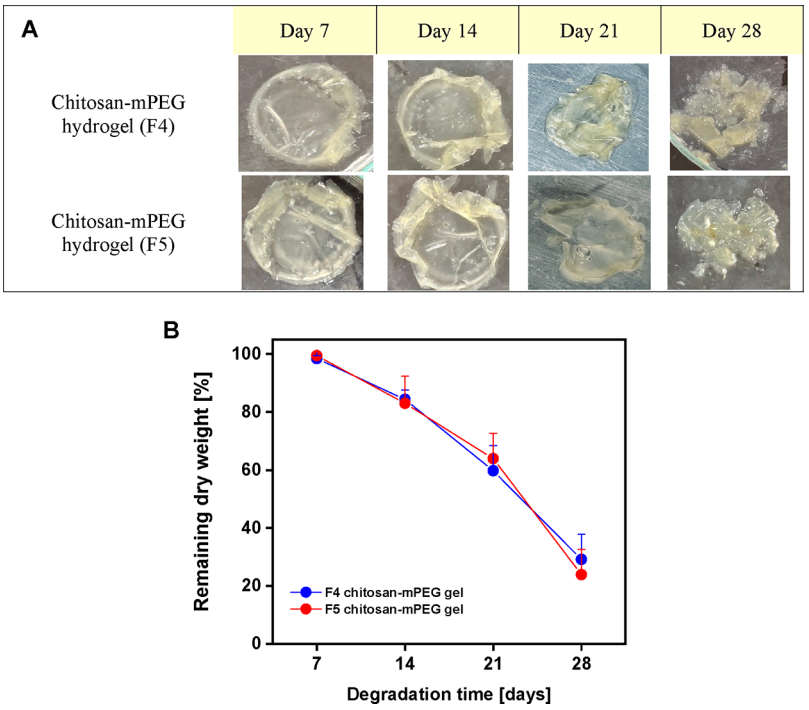

Figure 8. (A) Pictorial representation of the *in vitro* degradation behavior of F4 and F5 during 28 days of study in phosphate-buffered saline at pH 7.4. (B) Comparison of the *in vitro* degradation study of the F4 and F5 hydrogels during 28 days of study shows that the hydrogels erode slowly due to cross-linking between the polymers and degradation is a time-dependent phenomenon. Data points with error bars represent means ± standard deviations ($n = 3$). Photograph courtesy of "Fizza Mushtaq". Copyright 2022.

Both gels remained resistant for 3 weeks in phosphate-buffered saline. Still, during the fourth week, they degraded significantly, which may elaborate their biodegradability under physiologically relevant conditions and the environmental conditions that affect their stability while the slow erosion rate is due to strong bonding of the 3D hydrogel structure.[28]

2.3. Animal Study. In animal rat models, F4 and F5 chitosan−mPEG hydrogels were injected topically and effectiveness was compared with that of untreated wounded rats and the CMC 5%-treated and standard Flaminal Hydro-treated groups.

2.3.1. Wound Contraction Size. The diameter of the wound was measured on different days of treatments. Figure 9 shows that the standard treatment (Flaminal Hydro) significantly closed the wound on the 17th day, even if the wound was half closed on the seventh day. In comparison to the untreated group, the F4 chitosan−mPEG hydrogel group exhibited complete closure on the 25th day of treatment while the F5 chitosan−mPEG hydrogel group showed closed wound on the 19th day of treatment, which was almost very near to the standard.

2.3.2. Sequential Analysis of Phases of Wound Healing. In the study, the sequence of phases of wound healing was observed at day 0. All groups elicited a phase of hemostasis, which involved blockade of oozing of blood on day 2. Again, all groups scored 2 of intensive inflammation. The phase is

https://doi.org/10.1021/acsomega.3c04346
ACS Omega 2024, 9, 2145−2160

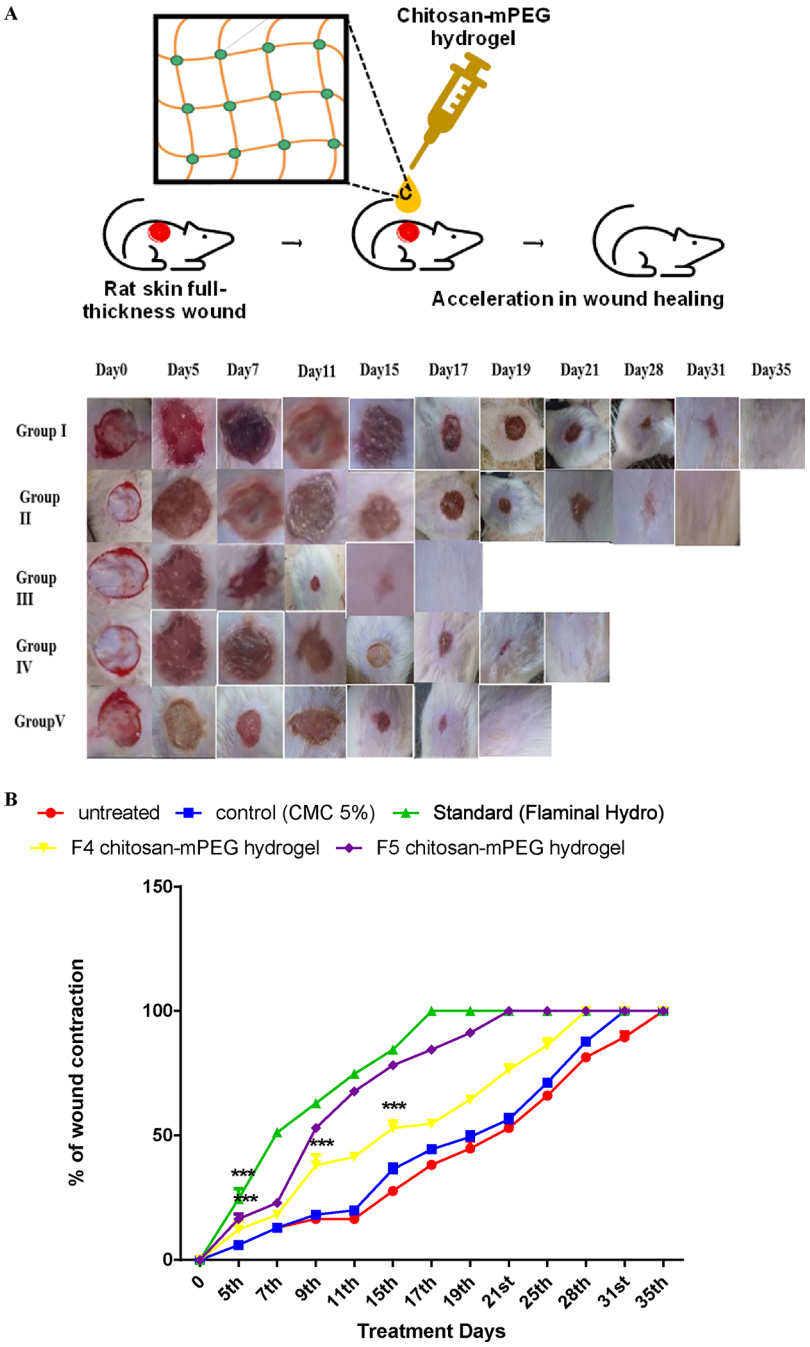

Figure 9. (A) Photographs of wounds of each group (group 1 untreated, group II treatment with CMC 5%, group III treatment with Flaminal Hydro, group IV treatment with F4 chitosan−mPEG hydrogel, and group V treatment with F5 chitosan−mPEG hydrogel. (B) Effect of treatments on wound contraction (percent) in the process of wound healing. ***$P < 0.001$ statistically significant difference in comparison with untreated group. Photograph courtesy of 'Madeeha Ashfaq & Fareeha Anwar'. Copyright 2023.

characterized by edema and vasodilation. Both the standard and F5 chitosan−mPEG hydrogel-treated groups scored 4 in phase of inflammation, while the F4 chitosan−mPEG hydrogel-treated group scored 3. The untreated group and control eradicated inflammation on day 11. The proliferative phase in the F5 chitosan−mPEG hydrogel-treated group appeared at day 7, while the F4 chitosan−mPEG hydrogel-treated group appeared at day 11 and the standard group completed its proliferative phase at day 7 and entered in a remodeling phase. However, the untreated and control groups took a prolonged time for wound contraction and revascularization. At day 17, the standard group reported wound maturation thoroughly and different chitosan hydrogel-treated groups scored wound maturation with a slight gap of one or 2 days. In contrast, the untreated and control groups showed wound maturation after 4 weeks (Table 2).

2.3.3. Clinical Assessment of the Wound Healing Process. The clinical sign of erythema scored intensively at day 0 in all groups of study. On days 5 and 7, only untreated and control groups exhibited mild erythema. The clinical indication of edema was significantly moderate in different-concentration chitosan hydrogel-treated groups as compared to the untreated and control groups at day 5 while the standard group appeared mild and absent on day 7. The exudate in all groups remained

https://doi.org/10.1021/acsomega.3c04346
ACS Omega 2024, 9, 2145−2160

Table 2. Effect of Treatments on Wound Healing[a]

	treatment groups				
days of treatment	untreated	control (CMC 5%)	standard (Flaminal Hydro)	F4 chitosan−mPEG hydrogel	F5 chitosan−mPEG hydrogel
day 0	1(0 + 1)	1(0 + 1)1	1(0 + 1)	1(0 + 1)	1(0 + 1)
day 2	2	2	2	2	2
day 5	5(2 + 3)	5(2 + 3)	9(4 + 5)	3	4
day 7	5(2 + 3)	5(2 + 3)	18(5 + 6+7)	4	16(4 + 5+6)
day 11	3	4	9	5	18(5 + 6+7)
day 17	5	5	10	18(5 + 6+7)	9
day 19	11(5 + 6)	11(5 + 6)		9	10
day 21	13(6 + 7)	13(6 + 7)		10	
day 28	8	9			

[a](A) Hemostasias (bleeding—0, clot formation—1). (B) Inflammation (intensive—2, moderate—3, mild—4) characterized by edema and vasodilation. (C) Proliferative phase (pebbled red tissue—5, wound contraction—6, revascularization—7). (D) Remodeling (mild—8, moderate—9, intensive—10) characterized by wound maturation.

Table 3. Clinical Examination of Effect of Treatments on Wound Healing[a]

		treatment days									
clinical features	treatment groups (n = 6)	D0	D2	D5	D7	D 11	D17	D19	D21	D28	D35
erythema	untreated	3	2	1	1	1	1				
	control	3	2	1	1	1	0				
	standard (Flaminal Hydro)	3	1	0	0	0					
	F4 chitosan-mPEG hydrogel	3	1	1	1	0	0				
	F5 chitosan-mPEG hydrogel	3	1	0	0	0	0				
edema	untreated	3	2	2	2	2	1	1			
	control	3	2	2	2	1	1	1			
	standard (Flaminal Hydro)	3	2	0	1	0					
	F4 chitosan-mPEG hydrogel	3	2	1	2	1	1				
	F5 chitosan-mPEG hydrogel	3	2	1	1	1	0				
exudate	untreated	3	3	2	2	2	2				
	control	3	3	2	2	2	2				
	standard (Flaminal Hydro)	3	2	1	1	0					
	F4 chitosan-mPEG hydrogel	3	2	1	2	1	1				
	F5 chitosan-mPEG hydrogel	3	2	1	1	1					
exudate color and consistency	untreated		5	4	4	4	4				
	control		5	4	4	4	4				
	standard (Flaminal Hydro)		4	4	4						
	F4 chitosan-mPEG hydrogel		4	4	4	4					
	F5 chitosan-mPEG hydrogel		4	4	4						
signs of granulation tissue	untreated								1	2	
	control								1	2	
	standard (Flaminal Hydro)				2	3					
	F4 chitosan-mPEG hydrogel				1	1	2	3			
	F5 chitosan-mPEG hydrogel			1	1	2	3				1
signs of infection	untreated	9	9	9	9	9	9		9		9
	control	9	9	9	9	9	9		9		9
	standard (Flaminal Hydro)	9	9	9	9	9		-			
	F4 chitosan-mPEG hydrogel	9	9	9	9	9	9		9		9
	F5 chitosan-mPEG hydrogel	9	9	9	9	9	9		9		9
re-epithelization	untreated	0	0	0	0	0	0				10
	control	0	0	0	0	0	0			10	
	standard (Flaminal Hydro)	0	0	1	1	2	3				
	F4 chitosan-mPEG hydrogel	0	0	1	2	2	3				
	F5 chitosan-mPEG hydrogel	0	0	1	1	1	2				

[a]Presence of erythema, edema, exudate and sign of granulation (0—absent, 1—mild, 2—moderate, 3—intensive), exudate color and consistency scored serous (4), serosanguineous (5), sanguineous (6), (5), sanguineous (6), purulent (7), signs of infection were scored as present (8); absent (9) and re-epithelization present (10); absent (11).

pinkish red in the healing process, indicating a healthy recovering wound, neither infectious nor necrotic. The exudate's color appeared serosanguineous only in untreated groups on the day of wound creation, while all other groups appeared with serous exudate in their inflammatory phase. Another important clinical symptom of the inflammatory phase

https://doi.org/10.1021/acsomega.3c04346
ACS Omega 2024, 9, 2145−2160

is the presence of infection. In this study, the chitosan hydrogel-treated group was marked absent in microbial invasion. For clinical features, a sign of granulation tissue in the F4 chitosan−mPEG hydrogel-treated group scored moderate and the F5 chitosan−mPEG hydrogel-treated group scored intensive at day 17 in contrast to the untreated and control groups, while the standard group showed a sign of granulation earlier. Re-epithelization appeared in each group at the end of their respective remodeling phase. In short, the F5 chitosan-mPEG hydrogel-treated group showed a sign of new epithelial layer earlier than the F4 chitosan-mPEG hydrogel-treated group (Table 3).

Initially, after injury hemostasis took place, both the F4 chitosan−mPEG hydrogel and F5 chitosan−mPEG hydrogel-treated groups showed hemostasis rapidly after wound creation. Taken together, this occurred at the molecular level due to the binding of positively charged chitosan polymers with negatively charged RBCs and platelets. Also, platelets plugged the damaged blood vessels and generated vasoconstrictor substances.[34] Likewise, a molecular basis was also exhibited in the surgical setting where the chitosan biopolymer was employed to stop the bleeding.[35] In the inflammatory phase, the chitosan hydrogel modulated the involved inflammatory elements and seemed effective in controlling inflammation. In clinical examination, the signs of erythema, edema, and exudate in the chitosan hydrogel-treated groups scored mild after the first week of injury.

2.3.4. Measurement of Tensile Strength. The tensile strength of the healed skin of all the groups was determined at the end of the study (Figure 10). The wound healed with

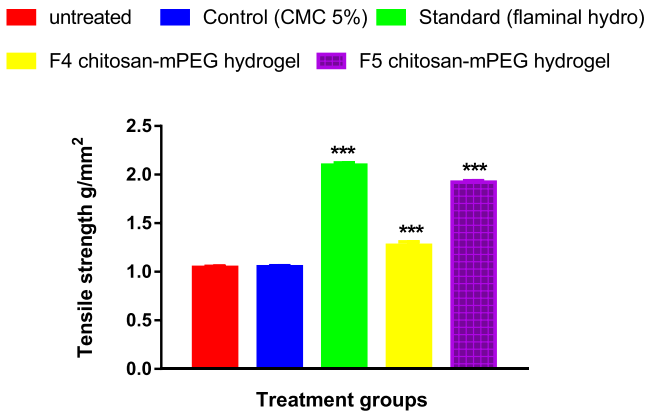

Figure 10. Improvement in tensile strength of all the groups of the study. ***$P < 0.001$ represents statistically significant difference in comparison with the untreated group.

the F4 and F5 chitosan−mPEG hydrogels showed significant results in contrast to the untreated and control groups ($P < 0.05$). The tensile strength of the standard group and the F5 chitosan−mPEG hydrogel group were recorded to be 2.097 ± 0.023 and 1.923 ± 0.034 g/mm, respectively, observed to be close to each other in contrast to the F4 chitosan hydrogel, which showed 1.273 ± 0.034 g/mm.

2.3.5. Hydroxyproline Estimation. Figure 11 shows that the content of hydroxyproline was found to be maximum in the standard group at 5.62 ± 0.03 mg/mL. The levels of hydroxyproline in both the F4 and F5 chitosan−mPEG hydrogel-treated groups were significantly increased in comparison to the untreated and control groups ($P < 0.001$).

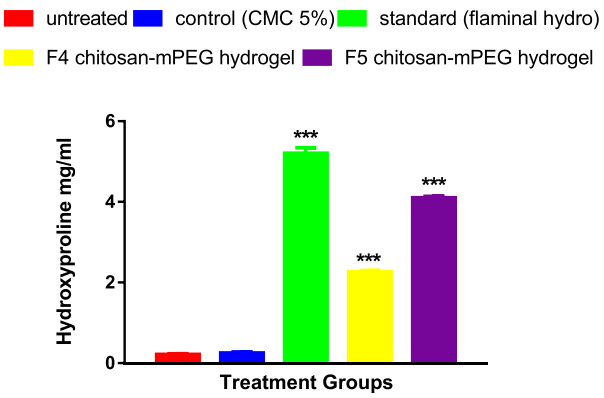

Figure 11. Hydroxyproline estimation in all postwound healing groups. ***$P < 0.001$ statistically significant difference in comparison with the untreated group.

Hence, the different concentrations of chitosan hydrogel appeared effective in the wound healing phenomenon by stimulating the formation of hydroxyproline, an important component of collagen of the skin.

2.3.6. Oxidative Stress. The levels of SOD and CAT were especially noted to be elevated in the standard group among other groups (Figure 12). The treatment group F5 chitosan−mPEG hydrogel also exhibited increased serum levels of SOD and CAT similar to the standard group. However, the SOD levels in the F4 chitosan−mPEG hydrogel-treated group was less statistically significant while CAT levels were statistically significant ($P < 0.05$) as compared to the standard group and the F4 chitosan−mPEG hydrogel-treated group, respectively. The CAT levels appeared raised in the CMC control group that received CMC 5% compared to the untreated group. The SOD levels in both the untreated and control groups were determined to be lowest in contrast to the standard and chitosan hydrogel-treated groups. Moreover, serum MDA levels were the highest in the untreated group and lowest in the standard group. Another oxidative stress indicator, nitric oxide levels, expressed least in the standard group, F4 chitosan−mPEG hydrogel-treated group, and F5 chitosan−mPEG hydrogel-treated group as compared to the untreated and control groups.

In open wounds, reactive oxygen species are secreted in the inflammatory phase. Concurrently, antioxidants are also enzymes present in body tissues for protection such as SOD (super dismutase) and CAT (catalase).[36] The different concentrations of chitosan hydrogels applied on acute wounds in the study showed elevated SOD and CAT levels compared to untreated wounds. The hydroxyl and amino functional groups protonated the ROS and upregulated the functions of ROS-detoxifying enzymes.[37] Excessive presence of another oxidative stress marker, malondialdehyde (MDA), affects the proliferative phase of healing. In this study, the F4 and F5 chitosan−mPEG hydrogel treatment significantly minimized the MDA level and avoided prolonged healing of wounds. The study on chitosan-based nanogels in wound healing also reported minimal MDA levels.[38]

Nitric oxide also showed significant antioxidant activity in the treatment of the F4 and F5 chitosan−mPEG hydrogel. Recently, study on chitosan hydrogel also demonstrated the prominent role of NO in diabetic wound healing in rabbits.[39] Hydroxyproline is a potential biomarker of collagen synthesis in healed granulated tissues.[40] In the study, wounds treated

https://doi.org/10.1021/acsomega.3c04346
ACS Omega 2024, 9, 2145−2160

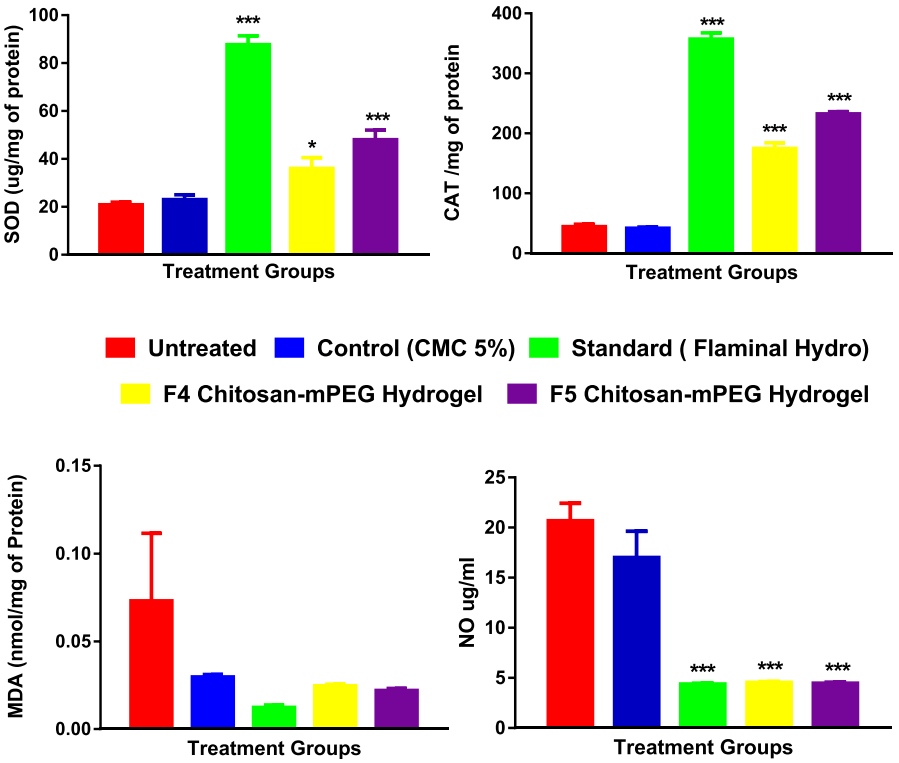

Figure 12. Effects on the levels of oxidative stress enzymes. ***$P < 0.001$ represents statistically significant difference in comparison with the untreated group while *$P < 0.05$ represents statistically significant difference in comparison with the untreated group.

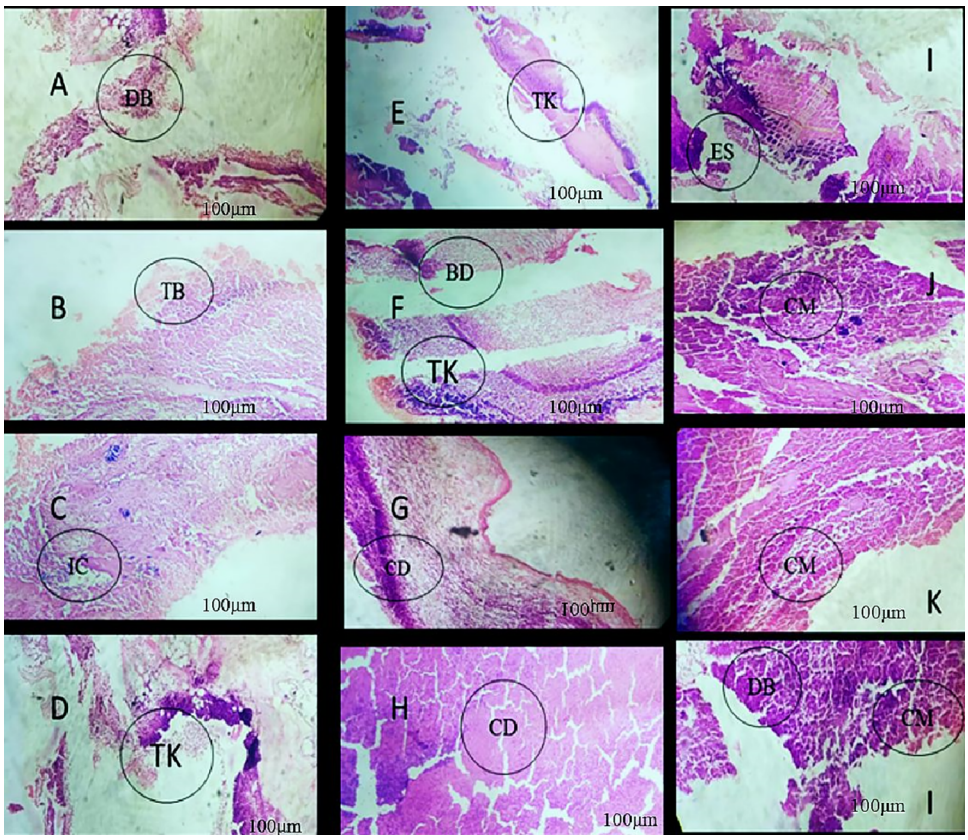

Figure 13. Presentation of histological observation of all of the groups of the study. (A) Group I = untreated group with (DB) defective borders. (B, C) Group III with (TB) thin borders and (IC) inflammatory cells. (D, E, H) Group IV with a gradual increase in (TK) thick epithelium and (CD) collagen deposition. (G, K) Group V with (TK) thick epithelium and (CM) collagen maturation. Photograph courtesy of 'Madeeha ashfaq & Fareeha Anwar'. Copyright 2023.

https://doi.org/10.1021/acsomega.3c04346
ACS Omega 2024, 9, 2145−2160

with the F5 chitosan−mPEG hydrogel demonstrated elevated levels of hydroxyproline in contrast to treatment with the F4 chitosan−mPEG hydrogel. The applied F5 chitosan−mPEG hydrogel primarily filled the wound bed with the granulated tissue. In histological analysis, excessive collagen deposition was observed in group E in Figure 13K. Additionally, signs of granulation scored moderate on day 11th and intensive on day 17th. It is also evident from the significant reduction of wound diameter on day 9th, day 11th, and day 15th and accelerated the rate closure of wound after remodeling at day 19th when compared to application of the F4 chitosan−mPEG hydrogel and untreated groups. Likewise, the study of photo cross-linked chitosan dressing also occluded the wound earlier.[41] Collagen fibers aligned in the remodeling phase and determined tensile strength.[42] The acute wounds healed with the F5 chitosan−mPEG hydrogel exhibited tensile strength near that of the standard group, which employed more breaking force to crack the reconstructed skin tissue. This finding is in agreement with the findings of wounds healed with chitosan and gelatin-based hydrogel.[43]

2.3.7. Histology Analysis. In the untreated group, injury was observed with defective borders, as shown in picture A of Figure 13 , while in the control group, the appearance of thin borders was noticed. This feature showed that both the untreated and control groups had damaged epithelial layers. Infiltration of inflammatory cells such as neutrophils was observed in the control group, indicating the second phase of wound healing. Concurrently, the F4 chitosan−mPEG hydrogel-treated group and F5 chitosan−mPEG hydrogel-treated group appeared with a thick-epithelium-marked granulation phase in pictures D and E, respectively. Moreover, the standard group demonstrated constricting borders with a thick epithelium in pictures F and G.

In histological analysis, limited inflammatory cells were seen in figure D and E of the chitosan−mPEG hydrogel-treated groups, which is in line with the results of other chitosan-based hydrogel research study used for wound healing.[44] Moreover, wound sites are excessively prone to microbial attack.[45] Previous data reported that chitosan has antimicrobial potential. It might be due to the interaction of positively charged functional groups of chitosan with negatively charged components of the cell wall of microbes.[46] A recent investigation of modified chitosan hydrogel preparation also explained the same antimicrobial activity in wound healing.[47]

Altogether, the results obtained in this study scientifically demonstrated gradual wound size contraction and acceleration of wound closure. Importantly, we observed clinical signs of wound repairing and significant improvement in tensile strength, with different concentrations of chitosan hydrogel cross-linked with methoxy propylene glycol. During the proliferation phase, the F5 chitosan−mPEG hydrogel showed increased hydroxyproline levels in chitosan−mPEG-treated groups, indicating excessive collagen deposition. From the authors' perspective, chitosan−mPEG hydrogels also exhibited antioxidant activity efficiently due to their structural feature that causes protonation of enzymes of redox reactions and inhibited the lipid peroxidation.

3. CONCLUSIONS

This study presents different concentrations of chitosan cross-linked with mPEG to develop an injectable chitosan−mPEG hybrid hydrogel employed to accelerate the wound-repairing process. To garner biologically relevant conclusions from the developed chitosan−mPEG hybrid hydrogel, the hydrogel was fully characterized in detail, which revealed biologically relevant stiffness, swelling, excellent cytocompatibility, antibacterial activity, and *in vitro* biodegradability. In contrast, a chitosan−mPEG hydrogel in-depth experimental study conducted on *in vivo* rat models demonstrated hemostasis soon after applying the hydrogel and acceleration in wound closure as compared to the control. In particular, the chitosan−mPEG hydrogel showed significant improvement in the healing of the acute wound. Taken together, it demonstrated earlier wound closure with considerable tensile strength. Ultimately, it caused a substantial rise in hydroxyproline levels in healed skin tissue, which efficiently dealt with oxidative stress. Based on the above experimental results, the injectable chitosan−mPEG hydrogel represents an on-demand material platform to apply on wounds where it promotes rapid wound healing. In summary, we believe that the chitosan−mPEG hybrid hydrogel has great potential in wound healing and should be further elucidated for extensive biomedical applications.

4. MATERIALS AND METHODS

4.1. Drugs and Chemicals. Chitosan (low molecular weight) was purchased from Sigma-Aldrich, USA. Methoxy polyethylene glycol acid (mPEG-COOH, M.W. 2000) was purchased from Advanced BioChemicals, LLC, USA. Beta (β)-glycerophosphate disodium salt hydrate, hydroxyproline, carboxymethyl cellulose, hydrochloric acid, potassium phosphate monobasic and dibasic, sodium phosphate monobasic and dibasic, pyrogallol, and sulfanilamide were purchased from Sigma-Aldrich, USA. Acetic acid (Fisher Scientific, USA), standard Flaminal Hydro (Flen Health, Belgium), Folin−Ciocalteu (Merck, Germany), trichloroacetic acid (Smart Lab, Indonesia), Chloramine-T solution, Ehrlich's reagent (Medilines, Pakistan), nutrient agar (HiMedia Laboratories, India), and all other chemicals used were of analytical grade.

4.2. Methodology. *4.2.1. Preparation of Injectable Chitosan−mPEG Hydrogel.* Chitosan was dissolved in 0.1 M acetic acid solution. Afterward, the viscous and clear chitosan solution was sterilized through moist heat sterilization at 121 °C temperature and 15 lb pressure for 15 min. Next, the mPEG-COOH after filtration was added to chitosan solution dropwise with continuous stirring under ambient conditions. The pH of the solution was adjusted to pH 7.2 by dropwise addition of an aqueous solution of β-glycerophosphate disodium salt under vigorous stirring in an ice bath. The solution was converted into chitosan−mPEG hybrid hydrogel after incubation (at 37 °C for 5 min). We hypothesize that mPEG acid would form an amide linkage with the available amino groups of chitosan as well as physical gelation of chitosan at neutral pH.

4.2.2. Characterization of Chemically Cross-Linked Chitosan Hydrogel. 4.2.2.1. Rheological Study. The developed chitosan hydrogels were rheologically analyzed to evaluate the hydrogel's viscoelastic properties. The samples were measured using a rheometer while being assembled with a cone and plate (time sweep rheology) or a plate and plate (frequency sweep rheology).[48,49] In short, the chitosan−mPEG hybrid hydrogel formulation was placed on the rheometer plate and time sweep rheology was performed at a frequency of 1 Hz to determine the change in storage and loss modulus over time.[50] Besides that, stress−strain rheology was also performed using a rheometer.

https://doi.org/10.1021/acsomega.3c04346
ACS Omega 2024, 9, 2145−2160

4.2.2.2. Swelling Behavior. The swelling property of hydrogels was assessed by immersion in phosphate-buffered saline (PBS) with pH 7.4 for 24 h. To this end, the chitosan hydrogels were freshly fabricated, hydrated in PBS, and subsequently weighed while later hydrated hydrogels were lyophilized for 24 h after freezing overnight and dried gel discs were considered. The dried gel discs were immersed in PBS under ambient conditions at different time points, allowing the hydrogels to take up liquid and swell. Thus, the dried weight and swollen weight were measured to determine the swelling ratio.[51] The swelling ratio was measured as follows.[52]

$$\text{swelling ratio} = \frac{W_s - W_d}{W_s} \times 100$$

where W_s is the swollen weight and W_d is the dry weight.

4.2.2.3. Leachability Study. The leachability study was conducted to identify unreacted starting materials and determine the gel fraction and porosity to deliver the desired contents within the given time. The leachability of hydrogels was measured by immersion in PBS having pH 7.4 for 24 h at 37 °C followed by lyophilization. The dried weight (D_w) of chitosan hydrogels after freeze-drying was calculated. Theoretical weight (T_w) was calculated (theoretical masses of chitosan and methoxy-PEG acid used in the reaction for hydrogel fabrication). Then, leachability was calculated by the following formula.[53]

$$\text{leachability} = \frac{T_w - D_w}{T_w}$$

4.2.2.4. Fourier Transform Infrared Spectrometry (FTIR). FTIR was performed to characterize the material's existence of specific chemical groups and chemical bonds. The infrared spectra of chitosan, mPEG acid, and mPEG-cross-linked chitosan gel were recorded on a bulk FTIR spectrometer (Bruker ALPHA) with an attenuated total reflection (ATR) accessory at room temperature. Samples were brought into contact with the ATR attachment in the sampling region. Spectra were collected at wavelengths ranging from 400 to 4000 cm^{-1}. Background subtraction was applied to all of the sample spectra. Before the next sample test, the sample cell was thoroughly cleaned with an alcohol and dried. Although all the materials were compatible with each other, no such significant changes were observed in chitosan, mPEG acid, and chitosan gel.

4.2.2.5. Thermal Gravimetric Analysis (TGA). The thermal stability of chitosan, mPEG acid, and chitosan−mPEG hydrogel was assessed using TGA (TA Instruments). In a typical analysis, the heating rate was set at 10 °C from 100 to 600 °C.

4.2.2.6. Cytocompatibility. Cytocompatibility of the chitosan−mPEG hydrogels was evaluated by WST (Rotitest Vital) assay at days 1, 2, and 3 after encapsulating L929 mouse fibroblast cells within the hydrogel matrix according to ISO 10993-5. To this end, L929 mouse fibroblast cells were cultured in a tissue culture flask with basic cell culture medium that consists of low-glucose Dulbecco's modified Eagle's medium (89%), fetal bovine serum (10%), and penicillin/streptomycin (1%).[54,55] In this experiment, L929 mouse fibroblast cells were trypsinized shortly before hydrogel fabrication. After trypsinization, cells were counted and mixed with warm and pH-adjusted (~pH 7.3) chitosan−mPEG solution in culture medium at a concentration of 100,000 cells per 50 μL in a 96-well plate to fabricate 3D cell-laden chitosan−mPEG hydrogel. The hydrogels were nourished with 100 μL of enriched culture medium and transferred to an incubator at 37 °C and 5% CO_2. The cell culture medium in the plate was replaced with fresh culture medium on alternate days. On the one hand, the 10,000 cells/well seeded in the well plate served as 2D control; on the other hand, chitosan−mPEG hydrogels without cells were taken as blank. In a typical experiment, hydrogels with and without cells as well as control were taken out at a defined time point, washed with PBS, and mechanically smashed to break the hydrogels after addition of 100 μL of culture medium. Afterward, 30 μL of water-soluble tetrazolium salt-8 (WST-8) reagent was added to each well containing hydrogels with and without cells as well as control, mixed, and incubated for 2 h. The absorbance was measured at 450 nm, and the experiments were performed in triplicate.

4.2.2.7. Antibacterial Activity Evaluation by the Agar Well Diffusion Method. The antibacterial activity of chitosan and chitosan−mPEG hydrogels against bacteria grown on culture was tested according to the ISO 22196:2011 standard. Briefly, the developed chitosan hydrogels were explored for their respective antibacterial activity against *Escherichia coli*(*E. coli*) as a representative bacterium.[56−58] In a typical experiment, a suspension of *E. coli*was spread with a cotton swab on sterile Petri dishes containing 25 mL of previously solidified sterile Luria−Bertani (LB) culture medium (Sigma-Aldrich St. Louis, Missouri, USA). Typically, the plate well diffusion method was used to envision the zones of inhibitions in solid culture medium. To this end, small circular cavities (8 mm) were punctured in the agar plate and afterward cavities were filled with 0.25 mL of chitosan or chitosan−mPEG hydrogels while distilled water was used as negative control in each plate. Subsequently, the plates were incubated at 37 °C for 24 and 48 h under aeration to allow microbial growth. At the defined time point, the plates were taken out of the incubator and zones of inhibitions were measured directly on the Petri dishes and average diameter of clear area was calculated. The results are represented as mean ± standard deviations of three independent plates replicates.

4.2.2.8. In Vitro Degradation. The *in vitro* degradation of the mPEG-cross-linked chitosan hydrogel was monitored by weight loss. First, the weighed quantity of hydrogel was placed into the phosphate buffer solution (0.1 M) and incubated at 37 °C for 4 weeks. Then, the buffer was replaced thrice a week with fresh buffer while at the defined time point, samples were collected from PBS, weighed, and dried and weighed again. The degradation rate of hydrogel or dry weight loss was determined by initial dry weight and weight at different degradation times, as shown in the following.[59]

$$\text{dry weight loss}(\%) = \frac{\text{initial dry weight} - \text{weight after degradation}}{\text{initial dry weight}} \times 100$$

4.3. Animal Study. *4.3.1. Experimental Animals.* Healthy albino rats of either sex weighed 150−200 g as used in this study. Animals were accumlitized 7 days in the lab before the start of the experiment. The temperature and humidity were maintained at 25 °C and 44% humidity, respectively, and in 12:12 light and dark cycles with access to water and feed. All the methods were approved by the research ethical committee of Riphah International University, Lahore, with an authorized

https://doi.org/10.1021/acsomega.3c04346
ACS Omega 2024, 9, 2145−2160

number of REC/RIPS-LHR2022053, following the National Institute of Health Guide for the Care guidelines and Use of Laboratory Animals.

4.3.2. Experimental Design. The rats were divided into five groups ($n = 7$). Group I was kept untreated, while group II was treated with vehicle control gel (CMC 5% gel). Group III was treated with the standard (Flaminal Hydro). Groups IV and V were treated with 0.3 and 0.4% chitosan hydrogel, respectively. All of the rats received excision-induced wounds on day 0 and received their treatments for days until the wound was closed. The day of wound closure was considered as the end of the study of the respective group. Each group received its respective topical treatment once a day.

4.3.3. Wound Creation. The rats were anesthetized with isoflurane 3.5% mixed with oxygen. The dorsal hair of each rat was shaved with an electric trimmer. The dorsal region was washed with alcohol. Afterward, a 1.5 cm-diameter wound was created with a surgical scissor on the dorsal side on rats.[60] Excessive bleeding was cleaned with an alcohol swab.

4.4. Wound Healing Evaluation Parameters. *4.4.1. Measurement of Wound Size.* The reduction in the size of the wound was calculated every day. The diameter of the wound was measured with a geometric compass and traced on translucent paper until the complete closure of wound. Wound contraction was calculated as percentage of original wound closure according to the following formula.

$$\%\ \text{of wound contraction} = \frac{\text{initial day wound size} - \text{specific day wound size}}{\text{initial day wound size}} \times 100$$

4.4.2. Sequential Evaluation of the Wound Healing Process. Wound healing comprises four stages. The phases of the wound healing process were analyzed and scored.

Phase I—hemostatic phase characterized by bleeding (0) and clot formation (1)

Phase II—inflammatory phase indicated by inflammation due to the presence of inflammatory cells and chemotactic factors (intensive—2, moderate—3, mild—4)

Phase III—proliferative phase identified by pebbled tissue (5), wound contraction (6), and revascularization (7)

Phase IV—remodeling phase demonstrated by wound maturation (mild—8, moderate—9, and intensive—10)

4.4.3. Clinical Assessment of Acute Wound. Healing of the wound was clinically examined by scoring. At each day, before treatment application, the clinical characteristics were observed.[61] Presence of erythema, edema, exudate, and appearance of granulation tissue were classified by the scores (0) absent, (1) mild, (2) moderate, and (3) intensive. Moreover, exudate color and consistency scored serous (4), serosanguineous (5), sanguineous (6), and purulent (7). Also, signs of infection were scored as present (8); absent (9) and re-epithelization as present (0); absent (1).

4.4.4. Measurement of Tensile Strength. Tensile strength demonstrates the mechanical firmness of the healed wound. The repaired skin tissues were excised from all the groups at the study's end. Tensile strength was calculated as force that caused a rupture in the newly formed skin and recorded in g/mm^2.[62] The following formula was used for calculation:

$$\text{tensile strength} = \frac{\text{breaking strength (g)}}{\text{cross section area of skin (mm}^2\text{)}}$$

4.4.5. Biochemical Analysis. 4.4.5.1. Hydroxyproline Estimation. Hydroxyproline is an important constituent of collagen. Its increased level is a marker of the effective healing of wounds. In this study, hydroxyproline levels were also estimated in each group of rats. Tissues were hydrolyzed in 6 N HCl for 4 h at 130 °C after drying in a hot air oven at 60 °C to a constant weight. The hydrolysates were then neutralized to pH 7.0. Afterward, 1 mL of Chloramine-T solution was added and incubated for 20 min. Reaction was terminated by the addition of 0.4 M perchloric acid and developed color with Ehrlich reagent at 60 °C. After thorough stirring, the samples' absorbance was measured at 557 nm. The hydroxyproline content in the tissue samples was calculated using a standard curve of the pure L-hydroxyproline.[63]

$$Y = 0.1124X + 0.545$$

4.4.5.2. Oxidative Stress Markers. The serum of the rats in each group was collected from blood obtained from cardiac puncture. The blood was centrifuged at 6000 rpm for 20 min. The supernatant serum was collected and used for the estimation of oxidative stress markers like SOD, CAT, MDA, and NO levels by using the previously published methods.[64−66] All of the experiments were performed in a triplicate manner.

4.4.6. Histological Analysis. From each animal group, wound tissues were collected and preserved in 10% formalin solution for histological evaluation. Sections of wound tissue specimens (about 5 μm thickness) were prepared by microtome and stained with hematoxylin and eosin (H&E) dye for histological examination. The magnification power kept 10× for observation.

4.5. Statistical Analysis. The data was expressed as mean ± standard error of the mean (SEM) and evaluated by analysis of variance (ANOVA). One-way and two-way ANOVA was followed by Dunnett's tests. OriginPro 2019b (OriginLab Corporation, Northampton, Massachusetts, U.S.A.) and GraphPad Prism software (GraphPad Software Inc., U.S.A.) were used for the analysis of all data. $P < 0.05$ was set for statistical significance.

■ ASSOCIATED CONTENT

Data Availability Statement

All data has been provided as original and no supplementary files are available.

■ AUTHOR INFORMATION

Corresponding Authors

Fareeha Anwar − *Riphah International University (R.I.U.), Riphah Institute of Pharmaceutical Sciences (RIPS), Lahore, Punjab 54000, Pakistan;* orcid.org/0000-0001-5097-8128; Phone: +92 333 8883251; Email: Fareeha.anwar@riphah.edu.pk

Iram Maqsood − *Riphah International University (R.I.U.), Riphah Institute of Pharmaceutical Sciences (RIPS), Lahore, Punjab 54000, Pakistan; Department of Pharmaceutics, School of Pharmacy, University of Maryland, Baltimore, Maryland 21201, United States*; Phone: +1(443)794-3120; Email: irammaqsood2@yahoo.com, imaqsood@rx.umaryland.edu

Authors

Fizza Mushtaq − *Riphah International University (R.I.U.), Riphah Institute of Pharmaceutical Sciences (RIPS), Lahore, Punjab 54000, Pakistan*

https://doi.org/10.1021/acsomega.3c04346
ACS Omega 2024, 9, 2145−2160

Madeeha Ashfaq − *Riphah International University (R.I.U.), Riphah Institute of Pharmaceutical Sciences (RIPS), Lahore, Punjab 54000, Pakistan*
Badarqa Tul Ayesha − *Riphah International University (R.I.U.), Riphah Institute of Pharmaceutical Sciences (RIPS), Lahore, Punjab 54000, Pakistan*
Hafiz Shahid Latif − *Fatima Jinnah Medical University, Lahore 54000, Pakistan*
Sadia Khalil − *Riphah International University (R.I.U.), Riphah Institute of Pharmaceutical Sciences (RIPS), Lahore, Punjab 54000, Pakistan*
Hafiz Shoaib Sarwar − *Faculty of Pharmacy, University of Central Punjab, Lahore 54000, Pakistan*
Muhammad Imran Khan − *Riphah International University (R.I.U.), Riphah Institute of Pharmaceutical Sciences (RIPS), Lahore, Punjab 54000, Pakistan*
Muhammad Farhan Sohail − *Riphah International University (R.I.U.), Riphah Institute of Pharmaceutical Sciences (RIPS), Lahore, Punjab 54000, Pakistan*

Complete contact information is available at: https://pubs.acs.org/10.1021/acsomega.3c04346

Author Contributions

#F.M. and M.A. contributed equally to the first authorship.

Author Contributions

Concept and planning, I.M., F.A., and B.T.A; investigation, F.M., M.A., and S.K.; methodology, I.M., F.A., F.M., M.F.S., H.S.S., M.I.K., and M.A; supervision, I.M., F.A., and B.T.A; writing—original draft, F.M. and M.A.; writing—review and editing, I.M. and F.A.

Notes

The authors declare no competing financial interest.

REFERENCES

(1) Venus, M.; Waterman, J.; McNab, I. Basic physiology of the skin. *Surgery (Oxford)* **2010**, *28*, 469−472.
(2) Herman, T. F.; Bordoni, B. *Wound classification*; StatPearls, (2020).
(3) Iyyam Pillai, S.; Palsamy, P.; Subramanian, S.; Kandaswamy, M. Wound healing properties of Indian propolis studied on excision wound-induced rats. *Pharm. Biol.* **2010**, *48*, 1198−1206.
(4) Stoica, A. E.; Chircov, C.; Grumezescu, A. M. Hydrogel dressings for the treatment of burn wounds: an up-to-date overview. *Materials* **2020**, *13*, 2853.
(5) Kojima, K.; Okamoto, Y.; Miyatake, K.; Kitamura, Y.; Minami, S. Collagen typing of granulation tissue induced by chitin and chitosan. *Carbohydr. Polym.* **1998**, *37*, 109−113.
(6) Ullah, K.; Sohail, M.; Murtaza, G.; Khan, S. A. Natural and synthetic materials based cmch/PVA hydrogels for oxaliplatin delivery: Fabrication, characterization, in-vitro and in-vivo safety profiling. *Int. J. Biol. Macromol.* **2019**, *122*, 538−548.
(7) Lee, C.-T.; Kung, P.-H.; Lee, Y.-D. Preparation of poly (vinyl alcohol)-chondroitin sulfate hydrogel as matrices in tissue engineering. *Carbohydr. Polym.* **2005**, *61*, 348−354.
(8) Kopecek, J. Polymer chemistry: swell gels. *Nature* **2002**, *417* (388−389), 391.
(9) Chirani, N.; et al. History and Applications of Hydrogels. *J. Biomed. Sci.* **2015**, *4*, 13−23.
(10) Liu, M.; et al. Injectable hydrogels for cartilage and bone tissue engineering. *Bone Res.* **2017**, *5*, 17014.
(11) Guvendiren, M.; Lu, H. D.; Burdick, J. A. Shear-thinning hydrogels for biomedical applications. *Soft Matter* **2012**, *8*, 260−272.
(12) Ahmad, Z.; et al. Versatility of hydrogels: from synthetic strategies, classification, and properties to biomedical applications. *Gels* **2022**, *8*, 167.
(13) Shoukat, H.; Buksh, K.; Noreen, S.; Pervaiz, F.; Maqbool, I. Hydrogels as potential drug-delivery systems: Network design and applications. *Ther. Delivery* **2021**, *12*, 375−396.
(14) Tibbitt, M. W.; Anseth, K. S. Hydrogels as extracellular matrix mimics for 3D cell culture. *Biotechnol. Bioeng.* **2009**, *103*, 655−663.
(15) Dai, T.; Tanaka, M.; Huang, Y.-Y.; Hamblin, M. R. Chitosan preparations for wounds and burns: antimicrobial and wound-healing effects. *Expert Rev. Anti-Infect. Ther.* **2011**, *9*, 857−879.
(16) Fu, J.; Yang, F.; Guo, Z. The chitosan hydrogels: from structure to function. *New J. Chem.* **2018**, *42*, 17162−17180.
(17) Labrude, P.; Becq, C. Le pharmacien et chimiste Henri Braconnot (Commercy 1780-Nancy 1855). *Rev. Hist. Pharm. (Paris)* **2003**, *91*, 61−78.
(18) Bektas, N.; Öenel, B.; Yenilmez, E.; Özatik, O.; Arslan, R. Evaluation of wound healing effect of chitosan-based gel formulation containing vitexin. *Saudi Pharm. J.* **2020**, *28*, 87−94.
(19) Hoemann, C.; Sun, J.; Legare, A.; McKee, M.; Buschmann, M. Tissue engineering of cartilage using an injectable and adhesive chitosan-based cell-delivery vehicle. *Osteoarthritis Cartilage* **2005**, *13*, 318−329.
(20) Harti, A. S.; Sulisetyawati, S. D.; Murharyati, A.; Oktariani, M.; Wijayanti, I. B. The effectiveness of snail slime and chitosan in wound healing. *Int. J. Pharma Med. Biol. Sci.* **2016**, *5*, 76.
(21) Craciun, A. M.; Morariu, S.; Marin, L. Self-Healing Chitosan Hydrogels: Preparation and Rheological Characterization. *Polymers* **2022**, *14*, 2570.
(22) Liu, K.; et al. Methoxy polyethylene glycol modification promotes adipogenesis by inducing the production of regulatory T cells in xenogeneic acellular adipose matrix. *Mater. Today Bio* **2021**, *12*, No. 100161.
(23) Li, X.; et al. Biodegradable MPEG-g-Chitosan and methoxy poly (ethylene glycol)-b-poly (ε-caprolactone) composite films: Part 1. Preparation and characterization. *Carbohydr. Polym.* **2010**, *79*, 429−436.
(24) Bubpamala, T.; Viravaidya-Pasuwat, K.; Pholpabu, P. Injectable poly (ethylene glycol) hydrogels cross-linked by metal−phenolic complex and albumin for controlled drug release. *ACS Omega* **2020**, *5*, 19437−19445.
(25) Zhu, J.; Li, F.; Wang, X.; Yu, J.; Wu, D. Hyaluronic acid and polyethylene glycol hybrid hydrogel encapsulating nanogel with hemostasis and sustainable antibacterial property for wound healing. *ACS Appl. Mater. Interfaces* **2018**, *10*, 13304−13316.
(26) Liu, S.; et al. Injectable and Degradable PEG Hydrogel with Antibacterial Performance for Promoting Wound Healing. *ACS Appl. Bio Mater.* **2021**, *4*, 2769−2780.
(27) Yilmaz Atay, H. Antibacterial activity of chitosan-based systems. *Funct. Chitosan: Drug Delivery Biomed. Appl.* **2019**, 457−489.
(28) Bhattarai, N.; Matsen, F. A.; Zhang, M. PEG-grafted chitosan as an injectable thermoreversible hydrogel. *Macromol. Biosci.* **2005**, *5*, 107−111.
(29) Tsao, C. T.; Hsiao, M. H.; Zhang, M. Y.; Levengood, S. L.; Zhang, M. Chitosan-PEG Hydrogel with Sol−Gel Transition Triggerable by Multiple External Stimuli. *Macromol. Rapid Commun.* **2015**, *36*, 332−338.
(30) Nesrinne, S.; Djamel, A. Synthesis, characterization and rheological behavior of pH sensitive poly(acrylamide-co-acrylic acid) hydrogels. *Arabian J. Chem.* **2017**, *10*, 539−547.
(31) Khodaverdi, E.; Ganji, F.; Tafaghodi, M.; Sadoogh, M. Effects of formulation properties on sol−gel behavior of chitosan/glycerolphosphate hydrogel. *Iran. Polym. J.* **2013**, *22*, 785−790.
(32) Ganji, F.; Vasheghani, F. S.; Vasheghani, F. E. Theoretical description of hydrogel swelling: a review. *Iran. Polym. J.* **2010**, *19* (5), 375−398.
(33) Yang, C.-H.; et al. Preparation and characterization of methoxy-poly(ethylene glycol) side chain grafted onto chitosan as a wound dressing film. *J. Appl. Polym. Sci.* **2015**, *132*, 42340 DOI: 10.1002/app.42340.

(34) Golebiewska, E. M.; Poole, A. W. Platelet secretion: From haemostasis to wound healing and beyond. *Blood Rev.* **2015**, *29*, 153−162.
(35) Sabab, A.; Vreugde, S.; Jukes, A.; Wormald, P.-J. The potential of chitosan-based haemostats for use in neurosurgical setting−Literature review. *J. Clin. Neurosci.* **2021**, *94*, 128−134.
(36) Schäfer, M.; Werner, S. Oxidative stress in normal and impaired wound repair. *Pharmacol. Res.* **2008**, *58*, 165−171.
(37) Si Trung, T.; Bao, H. N. D. Physicochemical properties and antioxidant activity of chitin and chitosan prepared from pacific white shrimp waste. *Int. J. Carbohydr. Chem.* **2015**, *2015*, No. 706259, DOI: 10.1155/2015/706259.
(38) Aslan, C.; Çelebi, N.; Deĝim, İ. T.; Atak, A.; Özer, Ç. Development of interleukin-2 loaded chitosan-based nanogels using artificial neural networks and investigating the effects on wound healing in rats. *AAPS PharmSciTech* **2017**, *18*, 1019−1030.
(39) Ahmed, R.; et al. Bone marrow mesenchymal stem cells preconditioned with nitric-oxide-releasing chitosan/PVA hydrogel accelerate diabetic wound healing in rabbits. *Biomed. Mater.* **2021**, *16*, No. 035014.
(40) Kumar Srivastava, A.; Khare, P.; Kumar Nagar, H.; Raghuwanshi, N.; Srivastava, R. Hydroxyproline: a potential biochemical marker and its role in the pathogenesis of different diseases. *Curr. Protein Pept. Sci.* **2016**, *17*, 596−602.
(41) Ishihara, M.; et al. Photocrosslinkable chitosan as a dressing for wound occlusion and accelerator in healing process. *Biomaterials* **2002**, *23*, 833−840.
(42) Mathew-Steiner, S. S.; Roy, S.; Sen, C. K. Collagen in wound healing. *Bioengineering* **2021**, *8*, 63.
(43) Ebhodaghe, S. O. A short review on chitosan and gelatin-based hydrogel composite polymers for wound healing. *J. Biomater. Sci. Polym. Ed.* **2022**, *33* (12), 1595−1622.
(44) Liu, H.; et al. A functional chitosan-based hydrogel as a wound dressing and drug delivery system in the treatment of wound healing. *RSC Adv.* **2018**, *8*, 7533−7549.
(45) Negut, I.; Grumezescu, V.; Grumezescu, A. M. Treatment strategies for infected wounds. *Molecules* **2018**, *23*, 2392.
(46) Ke, C.-L.; Deng, F.-S.; Chuang, C.-Y.; Lin, C.-H. Antimicrobial actions and applications of chitosan. *Polymers* **2021**, *13*, 904.
(47) Heedy, S.; Marshall, M. E.; Pineda, J. J.; Pearlman, E.; Yee, A. F. Synergistic antimicrobial activity of a nanopillar surface on a chitosan hydrogel. *ACS Appl. Bio Mater.* **2020**, *3*, 8040−8048.
(48) Vejjasilpa, K.; Maqsood, I.; Schulz-Siegmund, M.; Hacker, M. C. Adjustable Thermo-Responsive, Cell-Adhesive Tissue Engineering Scaffolds for Cell Stimulation through Periodic Changes in Culture Temperature. *Int. J. Mol. Sci.* **2022**, *24*, 572 DOI: 10.3390/ijms24010572.
(49) Kroschwald, L. M.; et al. Artificial Extracellular Matrices Containing Bioactive Glass Nanoparticles Promote Osteogenic Differentiation in Human Mesenchymal Stem Cells. *Int. J. Mol. Sci.* **2021**, *22*, 12819 DOI: 10.3390/ijms222312819.
(50) Wang, X.; et al. An Injectable Chitosan-Based Self-Healable Hydrogel System as An Antibacterial Wound Dressing. *Materials* **2021**, *14*, 5956.
(51) Begam, T.; Nagpal, A. K.; Singhal, R. A comparative study of swelling properties of hydrogels based on poly(acrylamide-co-methyl methacrylate) containing physical and chemical crosslinks. *J. Appl. Polym. Sci.* **2003**, *89*, 779−786.
(52) Zhang, K.; Yan, S.; Li, G.; Cui, L.; Yin, J. In-situ birth of MSCs multicellular spheroids in poly (L-glutamic acid)/chitosan scaffold for hyaline-like cartilage regeneration. *Biomaterials* **2015**, *71*, 24−34.
(53) Loth, T.; et al. Gelatin-based biomaterial engineering with anhydride-containing oligomeric cross-linkers. *Biomacromolecules* **2014**, *15*, 2104−2118.
(54) Wölk, C.; et al. Amphiphilic Functionalized Oligomers: A Promising Strategy for the Postfabrication Functionalization of Liposomes. *Adv. Mater. Interfaces* **2020**, *7*, No. 2001168.
(55) Nawaz, H. A.; et al. Injectable oligomer-cross-linked gelatine hydrogels via anhydride−amine-conjugation. *J. Mater. Chem. B* **2021**, *9*, 2295−2307.
(56) Maqsood, I.; Masood, M. I.; Nawaz, H. A.; Shahzadi, I.; Arslan, N. Formulation, characterization and in vitro evaluation of antifungal activity of Nystatin micro emulsion for topical application. *Pak. J. Pharm. Sci.* **2019**, *32*, 1671−1677.
(57) Shahzadi, I.; et al. Microemulsion Formulation for Topical Delivery of Miconazole Nitrate. *Int. J. Pharm. Sci. Rev. Res.* **2014**, *24*, 30−36.
(58) Maqsood, I.; et al. Preparation and in vitro evaluation of Nystatin micro emulsion based gel. *Pak J. Pharm. Sci.* **2015**, *28*, 1587−1593.
(59) Tan, R.; Niu, X.; Gan, S.; Feng, Q. Preparation and characterization of an injectable composite. *J. Mater. Sci.: Mater. Med.* **2009**, *20*, 1245−1253.
(60) Konca, M.; Korkmaz, M. Comparison of effects of administration of oral or topical boron on wound healing and oxidative stress in rats. *Kocatepe Vet. J.* **2020**, *13*, 11−18.
(61) Mota, M. R. L.; et al. Polysaccharide extract of Caesalpinia ferrea (Mart) pods attenuates inflammation and enhances the proliferative phase of rat cutaneous wounds. *Inflammopharmacology* **2022**, *30*, 1799−1810.
(62) Dwivedi, D.; Dwivedi, M.; Malviya, S.; Singh, V. Evaluation of wound healing, anti-microbial and antioxidant potential of Pongamia pinnata in wistar rats. *J. Tradit. Complementary Med.* **2017**, *7*, 79−85.
(63) Nagar, H. K.; et al. Pharmacological investigation of the wound healing activity of Cestrum nocturnum (L.) ointment in Wistar albino rats. *J. Pharm.* **2016**, *2016*, No. 9249040, DOI: 10.1155/2016/9249040.
(64) Fereiduni, E.; Ghasemi, A.; Elbestawi, M. Characterization of composite powder feedstock from powder bed fusion additive manufacturing perspective. *Materials* **2019**, *12*, 3673.
(65) Mir, N. T.; et al. Lawsonia Inermis markedly improves cognitive functions in animal models and modulate oxidative stress markers in the brain. *Medicina* **2019**, *55*, 192.
(66) Kirsch, G.; Abdelwahab, A. B.; Chaimbault, P. Natural and synthetic coumarins with effects on inflammation. *Molecules* **2016**, *21*, 1322.

https://doi.org/10.1021/acsomega.3c04346
ACS Omega 2024, 9, 2145−2160